Capillary electrophoretic separation of uncharged polymers using polyelectrolyte engines
Theoretical model

L.C. McCormick[a], G.W. Slater[a,*], A.E. Karger[b], W.N. Vreeland[c], A.E. Barron[c], C. Desruisseaux[d], G. Drouin[d]

[a]*Department of Physics, University of Ottawa, 150 Louis-Pasteur, Ottawa, Ontario K1N 6N5, Canada*
[b]*Applied Biosystems, Foster City, CA, USA*
[c]*Department of Chemical Engineering, Northwestern University, Evanston, IL, USA*
[d]*Department of Biology, University of Ottawa, Ottawa, Ontario K1N 6N5, Canada*

Abstract

We recently demonstrated that the molecular mass distribution of an uncharged polymer sample can be analyzed using free-solution capillary electrophoresis of DNA–polymer conjugates. In these conjugates, the DNA is providing the electromotive force while the uncharged polydisperse polymer chains of the sample retard the DNA engine with different amounts of hydrodynamic drag. Here we present a theoretical model of this new analytical method. We show that for the most favourable, diffusion-limited electrophoresis conditions, there is actually an optimal DNA size to achieve the separation of a given polymer sample. Moreover, we demonstrate that the effective friction coefficient of the polymer chains is related to the stiffness of the two polymers of the conjugate, thus offering a method to estimate the persistence length of the uncharged polymer through mobility measurements. Finally, we compare some of our predictions with available experimental results. © 2001 Elsevier Science B.V. All rights reserved.

Keywords: Mathematical modelling; Capillary electrophoresis; Polymers; DNA

1. Introduction

The polydispersity of a polymer solution is not easily determined using conventional methods such as gel permeation chromatography [1] and mass spectrometry [2]. Recently, we proposed and tested a new method to characterize the distribution of the varying degrees of polymerization of a water-soluble, uncharged polymer species [3]. The method is based on the idea that if a set of "engines" of uniform size and charge distribution is conjugated in

an unbiased way to all the polymer chains of the sample, one can in fact use free-solution capillary electrophoresis (CE) to study the distribution of polymer sizes. Indeed, the uncharged polymer then acts like a parachute, or "drag", and the retardation due to the drag molecule is directly proportional to its contour length. We called this method free solution conjugate electrophoresis (FSCE).

In our original paper [3], we showed the separation of each of 3400, 5000 and 20 000 nominal molecular mass poly(ethylene glycol) (PEG) samples using conjugated oligomeric DNA engines 20 and 35 bases long. Excellent quantitative results were obtained and compared with matrix-assisted laser de-

*Corresponding author.
E-mail address:* gslater@science.uottawa.ca (G.W. Slater).

sorption ionization time-of-flight (MALDI-TOF) MS data. Two results were particularly remarkable: (1) the 20-base DNA engine appeared to always give better results for a given set of experimental conditions, and (2) the effective friction coefficient of a PEG monomer was only about 14% of that of a DNA monomer. In this article, we derive the theory of FSCE and we examine these two results very carefully, i.e. we make predictions regarding the optimal engine size and the effective friction coefficient of the drag polymer.

Early experiments with FSCE-like separation techniques include the work of Stefansson and Novotny [4] who achieved separation of uncharged oligosaccharides through complexation with charged tags, and Bullock [5] who has also successfully separated uncharged PEG polymers through derivatization with phthalic anhydride. Although both of these early experiments were promising, they were not as precise and as easily controllable as the recent work of Vreeland et al., for example, in specifically varying the engine size. Nevertheless, the theory developed here could be adjusted for the experimental situations of the early studies.

Note that FSCE is essentially the complementary separation method to ELFSE, or end-labelled free-solution electrophoresis [6–8]. In ELFSE, a uniform (i.e., monodisperse) drag molecule is used to achieve the CE separation of a polydisperse polyelectrolyte sample. For instance, using streptavidin (a globular, uncharged protein) as the drag-label, we were able to sequence up to about 110 base long DNA samples in less than 20 min [8]. DNA sequencing using CE normally requires the use of a sieving polymer matrix (e.g., a gel or an entangled polymer solution) [9], but the extra drag added by the label allows us to achieve separation based only on the free-solution hydrodynamic properties of the conjugates. We have presented a theory of ELFSE in a recent paper [10], but this theory does not directly apply to FSCE since the latter is a method to resolve the drag label itself.

We will thus study the free-solution capillary electrophoresis of an uncharged sample composed of a polydisperse polymer solution conjugated to a monodisperse polyelectrolyte chain (Fig. 1). Hence, both components of the resulting complex are assumed to be flexible, water-soluble polymers. It would be quite easy to rewrite the theory for the
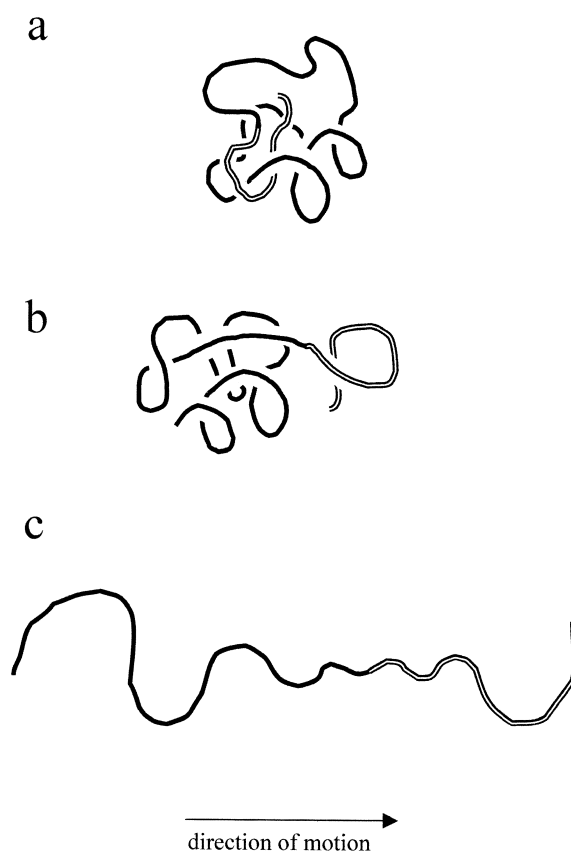

Fig. 1. Schematic representation of a block polyampholyte. The solid line shows the uncharged block while the double line shows the (shorter) charged block. (a) Equilibrium conformation; (b) segregation of the two blocks; (c) segregation and stretching of the blocks.

situation where the "engine" is a globular object such as a colloidal particle or a protein using the theoretical elements described in this article.

2. Theory for homogeneous charged–uncharged block copolymers

In this section, we examine the electrophoresis of a block copolymer consisting of a linear chain of charged monomers joined to a linear chain of uncharged monomers. The charged and uncharged blocks considered here are assumed to be homoge-

neous in the sense that they share the same flexibility (i.e. the same Kuhn length, b_K) and monomer size b.

2.1. The mobility

The mobility of polyampholytes was investigated by Long et al. [11]. Their theoretical results were fairly general, allowing for various charge distributions, including the specific case of our charged–uncharged complex. The theory takes into account the following five factors affecting the mobility of a polyampholyte in an approximately Gaussian conformation. (1) The force experienced by the charged monomers due directly to the electric field. (2) Hydrodynamic interactions that arise from the effect of the electric field on both the charged monomers and the counter ions surrounding them in the solution. (3) The tension along the polymer chain. (4) Thermal agitation. (5) The additional flow resulting from the previous two non-electrical factors. Factors 2 and 5 together comprise the ''flow field'' at the location of the nth monomer, due to the other monomers of the chain. Average equilibrium values of this flow field are utilized, since the focus is on the linear response of the chain. The mobility of a Gaussian and linear polyampholyte in a solution of high salt concentration was found to be a weighted average of the individual monomer mobilities, with the weight being essentially uniform and equal to $1/N$, where N is the total number of monomers. The weighting factor is actually somewhat higher for the last 10% of the monomers; e.g., it is about $1.5/N$ for the last 1% of the chain. This ''end-effect'' is a consequence of the greater hydrodynamic friction experienced, on average, by monomers at the end of the chain compared to those located inside the coil [11]. For sufficiently long charged sections, this effect can be neglected; however, as the number of charged monomers decreases, the small fraction of monomers that contribute with a greater weighting to the overall mobility may become important. Here we will analyze the situation where the end-effects can be neglected; a short discussion of the end-effects shall be presented in the Discussion section.

Hence, for a linear chain consisting of M_c charged monomers having a free electrophoretic mobility μ_0, and M_u uncharged monomers having no electrophoretic mobility, the overall mobility is simply an average wherein the weighting factor is approximately uniform:

$$\mu = \mu_0 \cdot \frac{M_c}{M_c + M_u} \tag{1}$$

This equation is valid so long as the two blocks retain significantly their equilibrium Gaussian conformational statistics [11] and remain hydrodynamically coupled, i.e., the two chains form a single random coil (see Fig. 1a). This condition of a single hydrodynamic unit is no longer met if the force with which the uncharged segment resists the movement via hydrodynamic drag is greater than the elastic, spring-like force which acts so as to maintain a single coiled conformation (see Fig. 1b). The drag force, i.e. the increased force of friction due to the uncharged block, depends on the electric field strength as this affects the speed which in turn determines the drag force. Hydrodynamic segregation can occur if the electric field strength and/or the hydrodynamic drag are too large. The conditions under which such decoupling may take place are typically extreme for electrophoresis; a calculation for the specific case of a DNA–streptavidin complex is presented in Ref. [10], wherein the critical electric field was indeed found to be very large ($E \approx 10$ kV/cm). Beyond the hydrodynamic segregation regime, an even greater difference between the electric force on the charged segment and the hydrodynamic drag force on the uncharged segment would result in a stretching of one or both blocks of the polyampholyte (Fig. 1c). We will not discuss these effects in this article since they are not relevant for currently available results and experimental setups.

2.2. The diffusion coefficient

We first note the classical result that the diffusion coefficient for a sphere of radius R, moving in a fluid, is given by the Stokes–Einstein equation [12]:

$$D = \frac{k_B T}{\xi} = \frac{k_B T}{6\pi\eta R} \tag{2}$$

where k_B is the Boltzmann factor, T is the absolute temperature, and η is the viscosity of the fluid. The radius which determines the coefficient of friction $\xi = 6\pi\eta R$ is not always as simple as for a hard

impermeable sphere; in the general case, the effective radius to be used is termed the hydrodynamic radius, R_H. For a Gaussian coil, the hydrodynamic radius is approximately two-thirds of the radius of gyration: $R_H \approx \frac{2}{3} R_G$ [13], where R_G can be obtained from the Kratky–Porod equation [14]. In the limit where the contour length l is much larger than the Kuhn length b_K, we obtain:

$$R_G^2 \simeq \frac{b_K l}{6} \qquad (3)$$

In order to simplify the calculations, we neglect excluded volume effects (such effects become important only for rather long polymer chains [14] and would only affect some quantitative aspects of our theoretical predictions). The contour length l is equal to the product of the total number of monomers and the distance b between two monomers: $l = (M_c + M_u)b$. The diffusion coefficient of our block polyampholyte is thus given by:

$$D = \frac{D_0}{\sqrt{M_c + M_u}} \qquad (4)$$

where D_0 is defined as:

$$D_0 \equiv \frac{kT}{4\pi\eta\sqrt{bb_K/6}} \qquad (5)$$

Note that this result is not affected by the presence of the electric field in the case of free-flow electrophoresis.

2.3. Optimal resolution for homogeneous complexes

In a recent paper by Vreeland et al. [3], two different charged chains (single-stranded, ss, DNA) were investigated for the optimal resolution of a DNA–polymer conjugate. The smaller of the two lengths (20 and 35 bases) was found to yield better resolution, for the same experimental parameters, leading to the apparent (but premature) conclusion that the smaller the charged chain utilized, the better the resolution. This can be anticipated to some degree, since the relative difference in mobility between consecutive uncharged chain lengths (M_u and $M_u + 1$) increases for decreasing numbers of

charged monomer ''engines'' (M_c), as can be seen from utilizing Eq. (1):

$$\frac{1}{\mu} \cdot \frac{\partial\mu}{\partial M_u} = \frac{1}{M_c + M_u} \qquad (6)$$

Hence the peak separation would benefit from shorter charged chain segments. However, there are competing effects which would indicate that a longer charged block could also benefit resolution; for example, a longer charged segment would lead to higher electrophoretic mobilities, allowing for less diffusion. It would also be a larger molecule, such that the diffusion coefficient would be smaller. Its increased speed, however, would also allow it less time to separate over the length of the capillary tube. Consequently, the capillary length and electric field strength, among other experimental parameters, could be expected to have an effect on the optimum length of the charged ''engine'' to be used.

We shall define the resolution factor R as the ratio of the final time width of two consecutive peaks, $\sigma_t(M) \simeq \sigma_t(M + 1)$, at the detector (expressed as the standard deviation of their assumed Gaussian distribution), to the difference in their elution times, $t(M)$:

$$R(M) = \frac{\sigma_t(M)}{t(M) - t(M-1)} \simeq \frac{\sigma_t(M)}{\partial t/\partial M} \qquad (7)$$

where $M = M_c + M_u = l/b$ is the total number of monomers. Note that by defining the resolution factor in this manner, the lower the value the better the resolution [8] since R has the units of monomer units (i.e., $R = r$ means that we can resolve molecules that differ by r monomers). To resolve a distribution of molecular sizes, we thus need $R \leq 1$.

The final spatial width includes a component due to the initial width, $\sigma_0(M) \simeq \sigma_0(M + 1)$, and a component due to the diffusion, which depends on the elution time, $t(M)$:

$$\sigma^2(M) = 2D(M)t(M) + \sigma_0^2(M) \qquad (8)$$

where the diffusion coefficient $D(M)$ is given by Eq. (4). For a peak velocity of $v(M) = \mu(M)E$, where E is the electric field, the time-width is related to the spatial width via:

$$\sigma_t(M) = \frac{\sigma(M)}{v(M)} = \frac{\sqrt{2D(M)t(M) + \sigma_0^2(M)}}{v(M)} \qquad (9)$$

The elution time $t(M)$ is simply the ratio of the effective length of the capillary (i.e. the distance to the detection point) L, to the velocity $v(M) = \mu(M)E$. Hence, the denominator of Eq. (7) can be written as:

$$\frac{\partial t(M)}{\partial M} = \frac{\partial}{\partial M}\left[\frac{L}{\mu(M)E}\right] \qquad (10)$$

and we can rewrite the resolution factor as:

$$R = \sqrt{\frac{2D(M)}{\mu^3(M)EL[(\partial/\partial M)(1/\mu)]^2} + \left[\frac{\sigma_0(M)}{\mu(M)L(\partial/\partial M)(1/\mu)}\right]^2} \qquad (11)$$

Since we are interested in the optimal resolution for chains with a set number of charged monomers, M_c, and differing uncharged chain lengths, M_u, we take the partial derivative of the mobility (Eq. (1)) with respect to M_u (i.e., $\partial/\partial M = \partial/\partial M_u$). Thus, using the equations for the diffusion coefficient and mobility (Eqs. (1) and (4)), the resolution becomes, for $M = M_c + M_u$:

$$R = \sqrt{\frac{2D_0}{\mu_0 EL} \cdot \frac{(M_c + M_u)^{5/2}}{M_c} + \frac{\sigma_0^2}{L^2}(M_c + M_u)^2} \qquad (12)$$

The optimal length of the charged section can now be obtained by solving the optimization condition $(\partial R/\partial M_c) = 0$. This yields the following fourth-order polynomial in M_c:

$$\Sigma_0^2 M_c^4 = \left(\tfrac{5}{2}\right)^2 \cdot (M_c + M_u)M_c^2 - 5(M_c + M_u)^2 M_c + (M_c + M_u)^3 \qquad (13)$$

where the only term representing the relevant experimental parameters is:

$$\Sigma_0 = \frac{\sigma_0^2 \mu_0 E}{LD_0} \qquad (14)$$

The exact solutions of this fourth-order polynomial are very long and hence are not given here; instead we present series solutions for the two limiting cases. Σ_0 is clearly a term representing the two factors which affect the final peak width: the

initial loading width ($\sim \sigma_0$), and the diffusion ($\sim D_0$). In fact, it is proportional to the critical length, $L_0 \equiv \sigma_0^2 \mu E/2D$, at which these two terms are equal [15]:

$$\Sigma_0 = \frac{L_0}{L} \cdot \frac{\sqrt{M_c + M_u}}{M_c} \qquad (15)$$

For typical experimental parameters (see Appendix A), Σ_0 may range from about 10^{-3} to 10^{+4}. In order to find a manageable solution for the optimal length of the charged segment, we will use series solutions for these two limits.

2.4. Optimal number of charged monomers for the diffusion-limited regime

First we note that in the limit of $\Sigma_0 = 0$ (i.e., negligible loading widths), Eq. (13) yields:

$$M_c = \tfrac{2}{3} \cdot M_u \qquad (16)$$

Hence, in this limit, the optimal number of charged monomers for the "engine" is not $M_c \to 1$, unlike the condition suggested by the data presented in Ref. [3]. Also of interest is that the optimal value of $\tfrac{2}{3}M_u$ does not depend on any system parameters such as the length of the capillary. A series solution around this value for M_c yields:

$$\frac{M_c}{M_u} \simeq \frac{2}{3} - \frac{8\sqrt{15}}{135} \cdot (\Sigma_0^2 M_u)^{1/2} + \frac{32}{225} \cdot (\Sigma_0^2 M_u) + \cdots \qquad (17)$$

This series agrees quite well with the full solution of Eq. (13), for the range of $0 \lesssim \Sigma_0^2 M_u \lesssim 1$, as can be seen in Fig. 2. The optimal value of M_c decreases smoothly from $\tfrac{2}{3}M_u$ when Σ_0 increases.

2.5. Optimal number of charged monomers for the injection-limited regime

A series solution for the region of large Σ_0 yields:

$$\frac{M_c}{M_u} \simeq \frac{1}{(\Sigma_0^2 M_u)^{1/4}} - \frac{1}{2(\Sigma_0^2 M_u)^{1/2}} + \cdots \qquad (18)$$

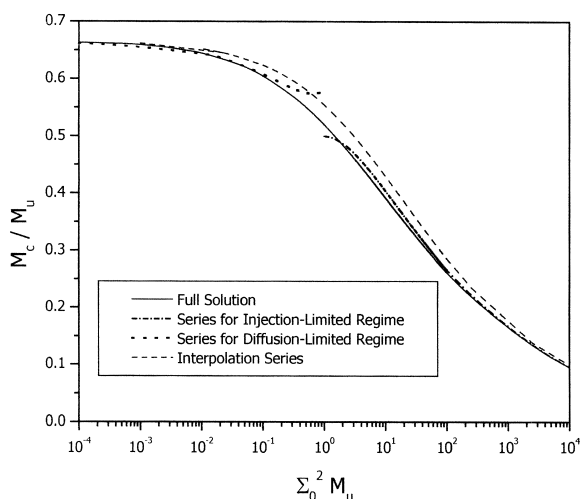Fig. 2 also displays this series solution. In contrast with the diffusion-limited regime, the optimal num-

Fig. 2. Ratio of the optimal engine size M_c to the size of the uncharged block M_u, vs. the expansion parameter $\Sigma_0^2 M_u$ which measures the impact of the injection width.

ber of charged monomers can now be quite small compared to M_u (of course, values smaller than unity are meaningless).

2.6. Discussion of FSCE for homogeneous block polyampholytes

Of course, one normally has a distribution of molecular sizes M_u to be analyzed. Therefore, what our analysis really suggests is that one should choose the engine size M_c to maximize the resolution near the peak of this distribution. However, since the resolution factor R increases with size M_u, it might be preferable to choose the engine size M_c to maximize the resolution for the largest polymers to be resolved (since the latter are the most difficult to resolve anyway). Let us call M_u^* this molecular size. The behaviour of the optimal M_c over the full range of Σ_0 is then approximated very well (see Fig. 2) by the following interpolating function:

$$M_c \approx \frac{\frac{2}{3} M_u^*}{\sqrt{1 + \frac{4}{9}(\Sigma_0^2 M_u^*)^{1/2}}} \qquad (19)$$

Perhaps the most interesting result is that the optimal engine size M_c for the separation of homogeneous molecules can be as large as $\frac{2}{3} \cdot M_u^*$. This nontrivial result comes from the competition between diffusion

and peak spacing. When the impact of the injection width is larger, as described by the parameter $\Sigma_0' \sim \sigma_0$, smaller engines are needed because more time (slower separations) is necessary in order to overcome the initial peak widths.

The optimal resolution (Eq. (12)) for the largest molecule to be resolved, in the limit of negligible loading width, is given by:

$$R(M_u^*)\big|_{M_c = 2/3 M_u^*} = \sqrt{\frac{D_0}{\mu_0 EL} \cdot \frac{5^{5/2}}{3^{3/2}} \cdot M_u^{*3/2}} \qquad (20)$$

Using the numerical values given in Appendix A, this can be rewritten as $R(M_u^*) \simeq (M_u^*/1300)^{3/4}$. This suggests that molecules up to $\simeq 1300$ monomers long could be resolved under these ideal conditions. Higher electric fields and longer capillaries can be used to increase this number. The corresponding elution time would then be (using Eq. (1)):

$$t(M_u^*) = \frac{L}{\mu(M_u^*)E} = \frac{5}{2} \cdot \frac{L}{\mu_0 E} \qquad (21)$$

Remarkably, the elution time of the M_u molecule is a universal multiple of the time $L/\mu_0 E$, the elution time of an unlabeled charged molecule. The latter, being less than 20 min for most experimental conditions, indicates that FSCE is a fairly fast separation process.

For the injection-limited regime where the optimal M_c approaches 1, however, the optimal resolution would be reduced to:

$$R(M_u^*)\big|_{M_c = 1} = \frac{\sigma_0}{L} \cdot (M_u^* + 1) \qquad (22)$$

The corresponding elution time would be (using Eq. (1)):

$$t(M_u^*)\big|_{M_c = 1} = (M_u^* + 1) \cdot \frac{L}{\mu_0 E} \qquad (23)$$

Although one can achieve fractionation of the sample using this limit, it is clearly not as good as the diffusion-limited situation discussed above. In particular, the time duration of the separation can be enormous.

In the next section, we generalize our analysis to treat inhomogeneous block copolymers made of blocks with different hydrodynamic properties.

3. Non-homogeneous charged–uncharged complexes

The equation for the mobility of a block poly-ampholyte, developed by Long et al. [11], assumes a homogeneous backbone, that is, charged and uncharged blocks having the same zero-field hydrodynamic properties; hence it will need to be adjusted for the case of non-homogeneous backbones. For example, Vreeland et al. [3] studied ssDNA–PEG conjugates. In order for their equation to be utilized, we visualize a regrouping of the monomers of both charged and uncharged chain segments into "super-monomer" units (called blobs) of uniform hydrodynamic radii (see Fig. 3), so as to "homogenize" the complex [10]. For example, three uncharged monomers could comprise a hydrodynamic blob equivalent to a blob made of five charged monomers. Hence the number of blobs, M_{B_i}, of type i ($i = $ c or u, for charged or uncharged, respectively) can be expressed as the total number of Kuhn lengths of type i, M_{K_i}, divided by the number of Kuhn lengths in each homogenized unit of type i, m_{K_i}:

$$M_{B_i} = \frac{M_{K_i}}{m_{K_i}} \tag{24}$$

with

$$M_{K_i} = \frac{l_i}{b_{K_i}} = \frac{M_i b_i}{b_{K_i}} \tag{25}$$

After redefining the blob-monomers, we can use Eq. (1) for the mobility of the complex made of M_{B_c} charged blobs (of mobility μ_{0_B}) and M_{B_u} uncharged blobs since all blobs are hydrodynamically equivalent. Using Eqs. (24) and (25), we then obtain:
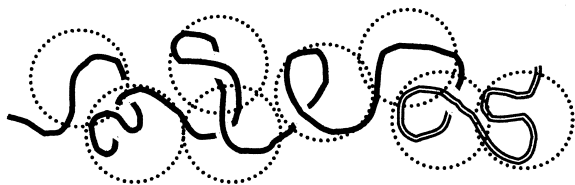

Fig. 3. Schematic representation of the blob construction for inhomogeneous backbones. We chose an extended molecular conformation for clarity.

$$\mu = \mu_{0_B} \cdot \frac{M_{B_c}}{M_{B_c} + M_{B_u}}$$

$$= \mu_{0_B} \cdot \frac{M_c}{M_c + M_u \cdot (m_{K_c} b_u b_{K_c} / m_{K_u} b_c b_{K_u})} \tag{26}$$

This equation can be further simplified by using the necessary equivalence of the hydrodynamic radii r_H of the charged and uncharged blobs:

$$r_{H_c} = r_{H_u} \tag{27}$$

From Section 2.2, we know that the hydrodynamic radius of a polymer chain of contour length l_i can be expressed in terms of its Kuhn length b_{K_i} as $r_{H_i} \simeq \frac{2}{3}(b_{K_i} l_i / 6)^{1/2}$. The total contour length within a blob of hydrodynamic radius r_H being given by $l_i = m_{K_i} b_{K_i}$, we obtain $r_{H_i} \simeq \frac{2}{3}(b_{K_i}^2 m_{K_i} / 6)^{1/2}$. Therefore, Eq. (27) leads to the important result:

$$\frac{m_{K_c}}{m_{K_u}} = \frac{b_{K_u}^2}{b_{K_c}^2} \tag{28}$$

and Eq. (26) can be expressed as:

$$\mu = \mu_{0_B} \cdot \frac{M_c}{M_c + M_u \alpha} \tag{29}$$

where we now introduce the microscopic parameter:

$$\alpha \equiv \frac{b_u b_{K_u}}{b_c b_{K_c}} \tag{30}$$

It is interesting to note that this is the only parameter that contains information about the chemistry of the two polymers. Moreover, this information is only relative since we find a ratio between various microscopic length scales (monomer sizes and Kuhn lengths).

Noting that the hydrodynamic radius of the block polyampholyte is $R_H = (R_{H_u}^2 + R_{H_c}^2)^{1/2}$, the diffusion coefficient from (Eq. (2)) becomes:

$$D = \frac{k_B T}{6\pi\eta\sqrt{R_{H_c}^2 + R_{H_u}^2}} = \frac{D_{0_c}}{\sqrt{M_c + \alpha M_u}} \tag{31}$$

where we used the fact that:

$$R_{B_i} \simeq \frac{2}{3} R_{G_i} = \frac{2}{3}\sqrt{b_i b_{K_i} M_i / 6}$$

and the definition:

$$D_{0_c} \equiv \frac{k_B T}{(4/\sqrt{6})\pi\eta\sqrt{b_c b_{K_c}}}$$

Utilizing the mobility and diffusion coefficients from Eqs. (29) and (31), Eq. (11) becomes, for non-homogeneous backbones:

$$R = \sqrt{\frac{2D_{0_c}}{\mu_{0_B} EL} \cdot \frac{(M_c + M_u\alpha)^{5/2}}{M_c\alpha^2} + \frac{\sigma_0^2}{L^2\alpha^2}(M_c + M_u\alpha)^2}$$

(32)

Taking the derivative of R with respect to M_c, and again setting it equal to zero, yields a fourth-order polynomial similar to that for homogeneous backbones (Eq. (13)):

$$\Sigma_{0_c}^2 M_c^4 = \left(\tfrac{5}{2}\right)^2 \cdot (M_c + M_u\alpha)M_c^2 - 5(M_c + M_u\alpha)^2 M_c$$
$$+ (M_c + M_u\alpha)^3$$

(33)

where $\Sigma_{0_c} \equiv \sigma_0^2 \mu_{0_B} E/LD_{0_c}$. Again the solution is similar to the homogeneous case, being closely approximated by:

$$\frac{M_c}{\alpha M_u} \approx \frac{2/3}{\sqrt{1 + (4/9)(\alpha M_u \Sigma_{0_c}^2)^{1/2}}}$$

(34)

Note that this solution is indeed equal to the corresponding equation (Eq. (19)) for the homogeneous condition $\alpha = 1$. As we can see, the microscopic parameter α simply rescales M_u: each charged monomer corresponds hydrodynamically to α uncharged monomers. This is the result of the fact that the monomers are no longer hydrodynamically equivalent.

Using Eq. (32), we can calculate the optimal resolution for the largest non-homogeneous block copolymer, which we again take to be of size M_u^*. In the limit of negligible loading widths, we obtain:

$$R(M_u^*)\big|_{M_c=(2\alpha/3)M_u^*} = \frac{1}{\alpha^{1/4}} \cdot \sqrt{\frac{D_{0_c}}{\mu_{0_B} EL} \frac{5^{5/2}}{3^{3/2}} \cdot M_u^{*3/2}}$$

(35)

and the corresponding elution time would be:

$$t(M_u^*) = \frac{L}{\mu(M_u^*)E} = \frac{5}{2} \cdot \frac{L}{\mu_{0_B} E}$$

(36)

which, remarkably, is the same as for the homogeneous case (Eq. (21)), and does not depend on the number of monomers or the nature of the polymers. Fig. 1 of Vreeland et al. [3] gives a factor of about 2.1 instead of 5/2, but their engine was not of optimal size. Using the numerical values described in Appendix A, we obtain $R(M_u^*) \simeq (M_u^*/680)^{3/4}$. For PEG, as used by Vreeland et al. [3], this predicts that the maximum molecular mass that we could resolve using FSCE, an optimal engine and these experimental conditions would be about 30 000 Daltons, close to what is suggested by these authors' results.

For the injection-limited regime where the optimal value of M_c approaches 1, the optimal resolution would be:

$$R(M_u^*)\big|_{M_c=1} = \frac{\sigma_0}{L} \cdot \left(M_u^* + \frac{1}{\alpha}\right)$$

(37)

while the corresponding elution time would be (using Eq. (29)):

$$t(M_u^*)\big|_{M_c=1} = (M_u^*\alpha + 1) \cdot \frac{L}{\mu_{0_B} E}$$

(38)

From Eqs. (35) and (37), it is evident that values of $\alpha < 1$ increase the resolution factor R, while $\alpha > 1$ results in smaller R's. Of course, the latter is preferable. Since $\alpha = b_u b_{K_u}/b_c b_{K_c}$, this indicates that one should choose the charged block such that it has a smaller monomer size b_c and/or a smaller Kuhn length b_{K_c} than the uncharged polymer sample that one wishes to separate. This is not trivial since most charged polymers tend to be rigid because of the extra electrostatic contribution to their Kuhn length.

4. Discussion

Free-solution conjugate electrophoresis has been shown to be a potential alternative to gel permeation chromatography and mass spectrometry for the analysis of the mass distribution of polydisperse polymer samples [3]. In this article, we have derived the basic theoretical framework for the development and optimization of FSCE. Three main elements were

needed: (1) a model for the electrophoretic mobility $\mu(M_u)$ of a linear polymer of degree of polymerization M_u end-conjugated to a polymeric charged engine of size M_c; (2) a model for the thermal diffusion coefficient $D(M_u,M_c)$ of these molecules; (3) a model to represent the effective friction coefficient of the two polymer blocks during the electrophoresis process. We demonstrated that the recent polyampholyte theory of Long et al. [11] could be generalized to treat this problem. One of the main results is that the effective frictional contribution of the polymer chains (described by the constant α) is proportional to the microscopic parameters (monomer size and chain stiffness) of both polymers. This readily suggests a new method to estimate the Kuhn length of uncharged polymers as a function of the Kuhn length of, for example, ssDNA under the same conditions. Our blob theory also explains why the FSCE electropherogram shows equally-spaced peaks (see Eqs. (1) and (29)), a most useful feature of this separation method [3].

It is interesting to use the recent results of ssDNA–PEG FSCE separations to test our theoretical model for the parameter α. Vreeland et al. reported that $\alpha = 0.138$ for their experimental conditions [3]. Using Eq. (30) and the fact that $b_{K_{ssDNA}} \approx 7$ nm and $b_{ssDNA} = 0.43$ nm [10], we find that $b_{K_{PEG}} \cdot b_{PEG} \approx 0.42$ nm^2. Since $b_{PEG} = 0.36$ nm, we get $b_{K_{PEG}} \approx 1.15$ nm (or ≈ 3 monomers), and a characteristic ratio $C_\infty = 3.2$, in fair agreement with the experimental value of $C_\infty = 3.8$. Incidentally, their value of $\alpha = 0.138$, together with Eq. (34), suggests that optimal results would be obtained, for the molecular mass 5000 PEG samples ($M_u = 114$), using a ssDNA label of size $M_c \leq (2\alpha/3)M_u = 10$ bases (the exact value depends on the importance of the injection width), while they used 20 and 35 base ssDNA engines.

Moreover, we determined how the resolution provided by FSCE depends on the actual size of the engine. For a diffusion-limited situation (always the best case scenario in separation science), there is actually an optimal engine size for a given polymer mass distribution. A general theory was also derived for a more general case where both the diffusion and the injection width limit the final resolution. Our analysis of these theoretical predictions indicates that much could indeed be gained by optimizing the

engine size M_c, increasing the microscopic parameter α (e.g., by changing the ionic strength of the buffer) and decreasing the experimental parameter Σ_0 (e.g., by increasing the field strength). Our theory thus introduces a systematic way to optimize FSCE.

Our model has neglected a number of effects that can modify its quantitative predictions to some extent, although none would modify its qualitative predictions. First, it must be noted that the mobility of the last charged blob, μ_{0_B}, can be slightly size dependent if the blob size is not large enough (e.g., the free-solution mobility of DNA is slightly size dependent below about 20 bases). This may introduce a small correction to our equations when the predicted optimal engine size is small. As we mentioned before, the theory of Long et al. [11] also introduces a small correction factor for both ends of the polymer. We also neglected excluded volume effects because they are often negligible for short polymers [14]; however, such effects can easily be added to the model. Finally, we must stress the fact that the version of the theory presented here assumed that the charged block was long enough to be represented by a Gaussian blob (i.e., we assumed that $M_c \gg b_{K_c}/b_c$); it is rather straightforward to modify the theory if the charged block is very rigid (e.g., one then has $r_{H_c} \sim M_c$).

Since FSCE, like ELFSE, is based on the hydrodynamic properties of macromolecules, anything that could alter the hydrodynamics of the analyte could potentially affect (negatively or positively) the performance of this new method. For example, very high field intensities could potentially lead to polymer deformation: this would greatly modify the effective frictional properties of both the engine and the polymer drag [10]. As discussed previously, this is not expected to happen under most circumstances. Of great interest would be the effect of branching and other nontrivial polymer structures. Indeed, the hydrodynamic properties of a non-linear macromolecule depend not only on the mass of the latter, but also on its precise configuration. We thus predict that FSCE could potentially be used to separate and characterize, for example, polymers of identical masses but different degrees of branching. The theory presented in this paper can be generalized to treat such cases.

Appendix A

In order to get some rough numerical predictions, we used the following "typical" ranges for the CE experimental parameters: $T \approx 300\text{--}340$ K, $\eta \approx 400\text{--}1000$ µPa s, $b_{K_{ssDNA}} \approx 5\text{--}10$ nm, $\sigma_0 = 0.1\text{--}10$ mm, $E \approx 100\text{--}1000$ V/cm, $\mu_0 \approx 1 \cdot 10^{-4}\text{--}5 \cdot 10^{-4}$ cm^2/V s, $L \approx 10\text{--}100$ cm. Finally, the ssDNA monomer size is $b_{ssDNA} \approx 0.43$ nm. Using these ranges, we find that Σ_0 may range from about 10^{-3} to 10^{+4}.

In addition, we used the following parameters to make predictions using Eqs. (20), (35) and (36): $D_0 = 7.0 \cdot 10^{-6}$ cm^2/s, $\mu_0 = 3 \cdot 10^{-4}$ cm^2/V s, $E = 300$ V/cm, $L = 40$ cm. We also used $\alpha \approx 0.138$, as determined by Vreeland et al. [3] for PEG.

References

[1] H.G. Barth, B.E. Boyes, C. Jackson, Anal. Chem. 70 (1998) 251R.
[2] A. Marie, F. Fournier, J.C. Tabet, Anal. Chem. 72 (2000) 5106.
[3] W.N. Vreeland, C. Desruisseaux, A.E. Karger, G. Drouin, G.W. Slater, A.E. Barron, Anal. Chem. 73 (2001) 1795.
[4] M. Stefansson, M. Novotny, Anal. Chem. 66 (1994) 1134.
[5] J. Bullock, J. Chromatogr. 645 (1993) 169.
[6] P. Mayer, G.W. Slater, G. Drouin, Anal. Chem. 66 (1994) 1777.
[7] C. Heller, G.W. Slater, P. Mayer, N. Dovichi, D. Pinto, J.-L. Viovy, G. Drouin, J. Chromatogr. A 806 (1998) 113.
[8] H. Ren, A.E. Karger, F. Oaks, S. Menchen, G.W. Slater, G. Drouin, Electrophoresis 20 (1999) 2501.
[9] P.G. Righetti (Ed.), Capillary Electrophoresis in Analytical Biotechnology, CR Press, New York, 1996.
[10] C. Desruisseaux, D. Long, G. Drouin, G.W. Slater, Macromolecules 34 (2001) 44.
[11] D. Long, A.V. Dobrynin, M. Rubinstein, A.J. Ajdari, J. Chem. Phys. 108 (1998) 1234.
[12] P. Munk, Introduction to Macromolecular Science, Wiley, New York, 1989.
[13] J. des Cloizeaux, G. Jannink, Les Polymères en Solution: leur Modélisation et leur Structure, Les Éditions de Physique, Paris, 1987.
[14] A.Y. Grosberg, A.R. Khokhlov, Statistical Physics of Macromolecules, AIP Press, New York, 1994.
[15] L. Bousse, C. Cohen, T. Nikiforov, A. Chow, A.R. Kopf-Sill, R. Dubrow, J.W. Parce, Annu. Rev. Biophys. Biomol. Struct. 29 (2000) 155.